Proceedings the 44th International School and Conference on the Physics of Semiconductors "Jaszowiec 2015", Wisła 2015

Magnetization of GaMnN Ceramics Prepared from Nanopowders by an Anaerobic Synthesis and High-Pressure High-Temperature Sintering

J.B. Gosk[a], M. Drygaś[b], J.F. Janik[b], S. Gierlotka[c], B. Pałosz[c] and A. Twardowski[d]

[a]Faculty of Physics, Warsaw University of Technology, Koszykowa 75, 00-662 Warszawa, Poland

[b]AGH University of Science and Technology, Faculty of Energy and Fuels, al. Mickiewicza 30, 30-059 Kraków, Poland

[c]Institute of High Pressure Physics, Polish Academy of Sciences, Sokołowska 29/37, 01-142 Warszawa, Poland

[d]Institute of Experimental Physics, Faculty of Physics, University of Warsaw, L. Pasteura 5, 02-093 Warszawa, Poland

Herein, we report a study on magnetic properties of GaMnN ceramics prepared by no additive high-pressure high-temperature sintering of a range of nanopowders, the latter made via an anaerobic synthesis method in the Ga/Mn bimetallic system at various nitridation temperatures and different levels of initial Mn concentration. Measurements of the magnetization as a function of temperature and magnetic field for the ceramics and parent nanopowders showed a typical paramagnetic behavior. Antiferromagnetic interactions between Mn-ions incorporated in the GaN lattice, GaMnN, were revealed and shown to be much stronger in the ceramics than in the respective nanopowders. In addition, in all of these materials an antiferromagnetic contribution originating from a residual Mn_2SiO_4 by-product was also observed. The highest calculated Mn concentration in the nanopowders reached 3.4 at.%. Complex mixtures of gallium nitride polytypes with multimodal particle size distributions in the nanosized range (small nano: 2–8 nm, large nano: 35–60 nm) were converted upon sintering to the single hexagonal GaN phase with average crystallite sizes of 40–80 nm and higher. For the optimal 700 °C-treated materials, the Mn concentration in the parent GaMnN nanopowder was 3.2 at.% whereas in the derived ceramics it amounted to 5.5 at.%. At the same time, contributions of the adventitious Mn_2SiO_4 by-product significantly decreased upon sintering.

DOI: 10.12693/APhysPolA.129.A-103

PACS: 75.50.Mm, 81.07.Wx, 81.07.–b

1. Introduction

Gallium nitride, GaN, a wide bandgap semiconductor has been intensively investigated in last decades both by synthetic chemists and theoreticians [1]. GaN suitably doped with a magnetic transition metal (TM = Mn, Fe, Cr, etc.) has been anticipated for many promising applications as a dilute magnetic semiconductor (DMS). However, despite numerous efforts DMS that are based on GaN tenaciously show too low T_C's to be considered for spintronics applications and making gallium nitride with a high Mn-content and specific physical properties poses still a great challenge for researchers. Looking back at all the numerous attempts to incorporate manganese at sufficiently high levels into the GaN lattice in the variety of materials forms (thin films, bulk samples or microcrystalline powders) and with various techniques that have been tried, one may consider the application of high-pressure high-temperature sintering of GaN/Mn nanopowders as a promising means to achieve the goal. If sintering is performed under conditions rendering GaN/Mn powders to recrystallize, the applied pressure–temperature conditions could favor, on the one hand, Mn-incorporation and, on the other hand, advantageous phase separation of residual contaminants, if any. In this regard, sintered GaN-based DMS ceramics prepared from nanopowders can, potentially, be a new convenient form of such materials for many challenging applications. This report is focused mainly on the magnetic properties of the novel attractive form of Mn-doped gallium nitride (labeled here as GaMnN) ceramics made of sintered nanopowders.

2. Samples

The method used to make GaMnN nanopowders was based on the anaerobic preparation of pure nanocrystalline gallium nitride GaN by ammonolysis of gallium tris(dimethyl)amide $Ga(NMe_2)_3$ (Me = CH_3) and nitriding pyrolysis of the resulting gallium imide by-product at elevated temperatures. In order to achieve the synthesis of Mn-doped materials, mixtures of $Ga(NMe_2)_3$ and $Mn[N(SiMe_3)_2]_2$ with predefined proportions of Mn/Ga at 5, 10, and 20 at.% Mn were first subjected to ammonolysis in refluxing ammonia followed by nitriding conversion as already reported by us [2]. In the present study, an optimal two-stage pyrolysis under an ammonia flow of the Ga/Mn amide-imide precursor isolated from the ammonolysis was applied: first stage at low temperature of 150 °C, 18 h and second stage at an elevated temperature, 4 h. In all cases, gray-beige to brownish final powders were synthesized. For the initial 10 at.% Mn precursor, the nitridation was carried out at 500, 700, and

900 °C to yield three respective products. For the 5 and 20 at.% Mn precursors, only the 900 °C-treatment was carried out.

The nanopowders were characterized by powder X-ray diffraction (XRD), the Fourier transform infrared (FT-IR) and Raman spectroscopy, X-ray fluorescence (XRF) elemental analysis, and scanning electron/energy dispersive X-ray (SEM/EDX) microscopy. The XRD data pointed out to the prevailing GaN lattice-based phases (hexagonal and/or cubic) in all nanopowders. Average crystallite sizes spanned from a few to a few tens of nanometers. The residues detected by other methods were either in very low proportions or, most likely, amorphous with the sole exception of the sample with the initial 20 at.% Mn which was nitrided at 900 °C where small amounts of the crystalline manganese silicates, tephroite and braunite, were observed. The air-sensitive by-products were artefacts of incomplete ammonolysis of the precursor mixtures and of the purposely applied Mn-excess.

The powders were sintered with no additives for 10 min in a high pressure toroid cell at 1000 °C under the pressure of 7 GPa using the methodology worked earlier for pure GaN nanopowders by some of us [3]. As a result, GaN/Mn black ceramic pellets were obtained, $D = 4$ mm, thickness 1–2 mm. The sintered ceramics were studied by XRD, FT-IR, and SEM/EDX. Detailed results of this investigation will be published elsewhere.

Magnetization of samples was measured as a function of magnetic field (up to 7 T) and temperature (2–400 K) using a SQUID magnetometer. For all the samples, a diamagnetic contribution of the host GaN material was taken into account.

3. Results

The XRD patterns generally supported recrystallization and grain growth during the high-pressure high-temperature sintering with an exception of one product that was made from the powder with the initial 20 at.% Mn and which was nitrided at 900 °C; in this case, the average crystallite size in the ceramics, 20 nm, was lower than in the substrate nanopowder, 35 nm, most likely due to a thinning/diluent effect. In all cases, the GaN-based phase was hexagonal. In addition, some ceramics contained small to moderate quantities of manganese silicates, blythite or tephroite, and some showed also diamagnetic α-gallium oxide (α-Ga_2O_3) or γ-gallium oxynitride (γ-$Ga_2(O,N)_3$); these by-products could be linked to the related residues in the substrate powders. SEM images showed that the ceramics from the 900 °C-treatment were the most homogeneous whereas the pellets from the powders prepared at lower temperatures included large crystallites embedded in the matrix of fine particles. The relevant FT-IR spectra supported the presence of GaN and some Mn–N–Si–C-related by-products in the investigated ceramics.

Generally, all measured samples, both the substrate nanopowders and the derived ceramics, show an overall paramagnetic (PM) contribution accompanied by some antiferromagnetic (AFM) component. There are no indications for the presence of disadvantageous ferromagnetic (FM) precipitates/clusters, commonly occurring in GaMnN grown by other techniques [3, 4]. The magnetic features of the parent nanopowders are similar to those observed earlier by us in a related study for a range of Ga/Mn compositions [2]. As before, we ascribe the PM contributions to Mn-ions incorporated in the GaN lattice, GaMnN, whereas the AFM contribution to an antiferromagnetic by-product. It could be inferred from the current magnetization data and substantiated by the earlier study that the most likely candidate for the latter is manganese orthosilicate Mn_2SiO_4 — an oxidation product of Mn excess-related residues. One needs to note that residual quantities of the diamagnetic phases, i.e., γ-$Ga_2(O,N)_3$ and α-Ga_2O_3 were also found by XRD in the ceramics 5%Mn 900 °C, 10%Mn 900 °C, and 10%Mn 500 °C, respectively. The representative results for the 700 °C-nitrided nanopowder (initial 10 at.% Mn) and the resultant ceramics are shown in Fig. 1.

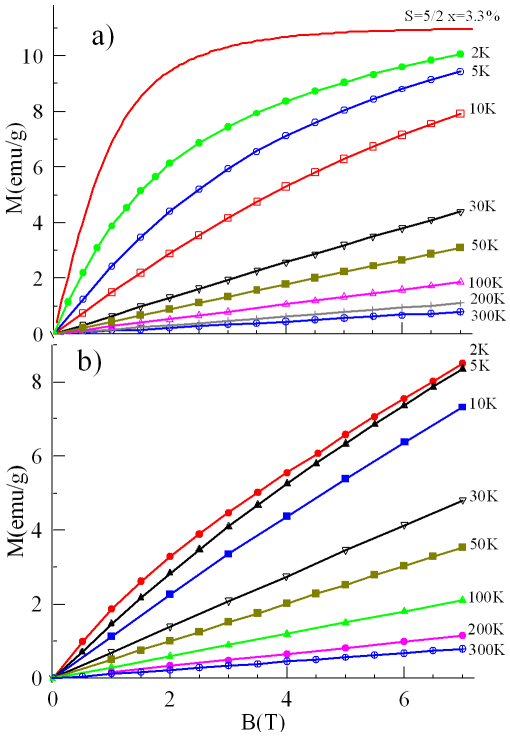

Fig. 1. Magnetization as a function of magnetic field at different temperatures for GaMnN materials labeled 10%Mn 700: a) substrate nanopowder; the solid line represents a reference Brillouin function with $S = 5/2$ and Mn-content $x = 3.3$ at.%, b) sintered ceramics.

The magnetization of the nanopowders reveals a typical paramagnetic, Brillouin-like behavior: it tends to saturate with increasing magnetic field at the lowest temperatures whereas at higher temperatures (T >50 K) it is linear with magnetic field. However, at $T = 2$ K it appears to saturate significantly slower than expected for non-interacting Mn-ions in d^5 configuration (see the ref-

erence Brillouin function for $S = 5/2$, $x = 3.3$ at.% Mn and $T = 2$ K in Fig. 1a). The observed slow saturation at the lowest temperatures can be assigned to AFM interactions between Mn-ions in the GaN lattice as well as to an additional linear contribution originating from the AFM by-product, i.e., Mn_2SiO_4 (T_N =50 K) [5]. We assumed for both the nanopowders and the ceramics the most frequently observed in Mn-doped gallium nitride materials [6, 7]* $Mn^{2+}(d^5)$ charge state. The evidence for the AFM contribution can also be found in high temperatures data (Fig. 1, $T = 100$, 200, and 300 K) where a characteristic linear offset directly indicates an AFM component in the total measured magnetization [2].

The magnetic behavior of all sintered ceramics is quite different from that of the related substrate nanopowders. It is well exemplified by the magnetization data for the sintered sample labeled 10 at.% Mn 700 °C (Fig. 1b). When comparing the measurements for the substrate nanopowder and the ceramics derived from it one notes that the high temperature data are essentially quite similar for both types of samples, whereas the low temperature data are significantly different. In the case of the ceramics, the magnetization only slowly saturates with magnetic field (*cf.* data for $T = 2$, 5, and 10 K in Fig. 1b). This may result from stronger Mn–Mn AFM interactions in GaMnN and, partly, from a linear response of the AFM phase contributing to the total magnetization of the ceramics. Since the high temperature data are very similar for both types of samples (*cf.* data for $T = 50$, 100, 200, and 300 K in Fig. 1a and b), the low temperature difference may be due to a stronger effect of Mn–Mn interactions, which in turn may suggest a higher Mn-concentration in the sintered ceramics.

Another way to demonstrate the AFM-type contribution to the total magnetization as well as to investigate interactions between magnetic centers in the PM phase is to plot MT as a function of temperature T at constant magnetic field. We recall that for a purely paramagnetic, non-interacting system of magnetic moments MT should not depend on T if temperature is not very low. Moreover, the constant value of MT is related to the number of magnetic centers in the system [2]. On the other hand, the interactions between magnetic centers in a PM phase result in bending of the MT vs. T curve — downwards for AFM interactions and upwards for FM interactions. Such bending is, therefore, recognized as a signature of interactions between magnetic centers in the PM phase.

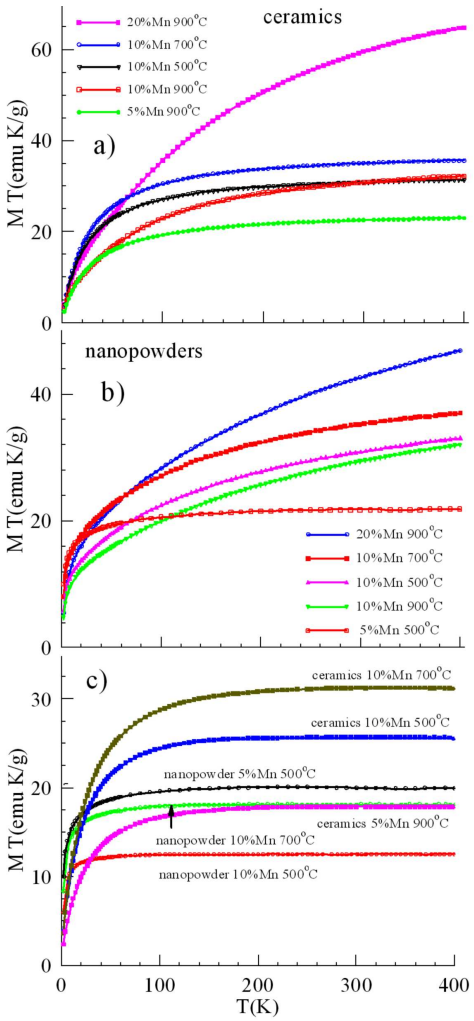

Fig. 2. MT as a function of temperature T at $B = 1$ T for 500, 700, and 900 °C-derived materials: a) ceramics with 5, 10, and 20 at.% Mn; b) selected nanopowders with 5, 10, and 20 at.% Mn; c) MT *vs.* T for 500 and 700 °C-derived nanopowders and related ceramics after subtraction of the AFM contribution for Mn_2SiO_4.

Magnetization measured as a function of temperature, represented in the MT vs. T coordinate system, for all sintered samples and four substrate nanopowders is depicted in Fig. 2. For comparison purposes, also included is a curve for a nanopowder with the initial 5 at.% Mn, which was nitrided at 500 °C. From the analysis of the curves it follows that the overall lowest PM contributions coupled with the highest AFM contribution among the

*In the case of potential Mn^{3+} (d^4) magnetic centers, GaMnN crystals should show magnetic anisotropy, which was demonstrated by Gosk et al. [7]. However, in that work such centers were observed in the GaMnN:Mg single crystals that were additionally co-doped with magnesium. Generally, for randomly oriented particles of GaMnN nanopowders with the assumed Mn^{3+} (d^4) magnetic centers the magnetization vs. B curves should reveal much slower saturation than the Brillouin function for $S = 5/2$. Such a situation was encountered by us in other related materials of this type, i.e., GaN nanopowders surface-doped with Mn-centers and the account will be published elsewhere. In the current study and the low temperatures data for the ceramics, the magnetic anisotropy alone could not account for the hardly saturating M vs. B curves (Fig. 1b). Namely, the saturation of magnetization averaged out over all orientations of grains with respect to the magnetic field (configuration d^4) is more pronounced than experimentally observed. On a final note, even if one assumes the Mn^{3+} (d^4) configuration in the GaMnN phase, this does not change much the major conclusions of the study whereas the estimated Mn-contents will be proportionally lower.

samples are displayed by the ceramics 20%Mn 900 °C. Interestingly, the parent nanopowder 20%Mn 900 °C shows the very similar magnetic characteristics in relation to other nanopowders (Fig. 2b, [2]). A relatively high AFM contribution is also shown by the ceramics 10%Mn 900 °C. As seen in Fig. 2a, the curves MT vs. T for the ceramics 10%Mn 700 °C, 10%Mn 500 °C, and 5%Mn 900 °C have very similar shapes which only slightly continue to grow with temperature for $T > 200$ K pointing out to relatively low contributions of the AFM phase. The ceramics 10%Mn 700 °C appears to show the highest PM contribution among the relevant samples.

Applying the procedure described in [2], one can subtract a contribution of the AFM phase from the measured total magnetization to get a contribution of the paramagnetic GaMnN phase. The result of such subtraction for the ceramics 10%Mn 500 °C, 10%Mn 700 °C, and 5%Mn 900 °C and for nanopowders nitrided at 500 and 700 °C is shown in Fig. 2c. Two important facts could be inferred from the data. First, let us compare the two almost overlapping curves in the range $T > 200$ K, i.e., for the nanopowder 5%Mn 500 °C and the ceramics 10%Mn 700 °C. For the latter, a stronger downward bending ($T < 200$ K) of MT vs. T curve points out to a stronger AFM effect thus confirming the findings of the M vs. B measurements. Second, in the group of low temperature nanopowder-derived ceramics the Mn concentration in GaMnN is about 1.6 times higher than in the parent nanopowders (*cf.* the relevant values of the high temperature MT range in Fig. 2c). We recall that the highest Mn concentration among all nanopowders was found for the 5% Mn 500 °C material that, at the same time, is characteristic of the lowest AFM contribution among all investigated samples (Fig. 2b, [2]). However, the relatively low nitridation temperature of 500 °C results also in the reactive nanopowders prone to oxidation in air. The nitridation at 700 °C and higher temperatures appears to yield more chemically stable products and still high levels of incorporated Mn. In order to create advantageous conditions for the highest possible Mn-contents, we used also the bimetallic precursor mixtures with extremely high Mn-contents of 20 and 50 at.% Mn, the data for the latter composition not discussed in this report. Regardless of the initial Mn-content, the resulting nanopowders do not show increased proportions of Mn in the paramagnetic GaMnN whereas contain larger quantities of the antiferromagnetic Mn_2SiO_4 by-product.

The MT values corresponding to higher temperatures, where MT vs. T is horizontal, should allow for estimations of the Mn-content in the paramagnetic GaMnN phase. To do this one needs to know the mass of the phases. In the particular case when the mass of other than Mn_2SiO_4 by-products (e.g., not detected by XRD amorphous residual phases) could be neglected the Mn concentration in GaMnN might be determined [2]. As mentioned before, in three ceramics, i.e., 5%Mn 900 °C, 10%Mn 900 °C, and 10%Mn 500 °C, in addition to GaMnN and manganese silicates which constitute the dominant phases in all materials, residual quantities of the diamagnetic components were also detected. This factor contributes to an additional error in calculations. Eventually, the estimated Mn-contents in the ceramics 10%Mn 500 °C, 10%Mn 700 °C, and 10%Mn 900 °C are 4.5, 5.5, and 3.2 at.%, respectively. Specifically, for the nanopowder 10%Mn 700 °C and the resultant ceramics important changes of magnetic properties due to the application of high-pressure high-temperature conditions should be noticed. Upon sintering, the Mn-content in the GaMnN phase increased from 3.2 to 5.5 at.% whereas the proportion of the residual Mn_2SiO_4 by-product decreased from 8.1 wt% to 1.3 wt%.

4. Conclusions

The sintering process results in the increased Mn-contents in the major crystalline GaMnN phase of the ceramics. Such an outcome suggests that under the applied conditions some available Mn-ions, e.g., from the AFM phase(s) in the nanopowders have diffused to the original paramagnetic GaMnN phase. A net magnetization effect is the observed relative decrease of the AFM contribution and, simultaneously, increase of Mn concentration in the PM contribution in the ceramics.

Acknowledgments

Study was funded by the Polish National Science Center NCN, Grant No. 2011/01/B/ST5/06592.

References

[1] (a) T. Dietl, H. Ohno, *Rev. Mod. Phys.* **86**, 187 (2014) and references therein; (b) T. Jungwirth, J. Wunderlich, V. Novak, K. Olejnik, B.L. Gallagher, R.P. Campion, K.W. Edmonds, A.W. Rushforth, A.J. Ferguson, P. Nemec, *Rev. Mod. Phys.* **86**, 855 (2014); (c) A. Hirohata, K. Takanashi, *J. Phys. D Appl. Phys.* **47**, 193001 (2014); (d) S.S. Khludkov, I.A. Prudaev, O.P. Tolbanov, *Russ. Phys. J.* **55**, 903 (2013); (e) R. Buonsanti, D.J. Milliron, *Chem. Mater.* **25**, 1305 (2013).

[2] (a) M. Drygas, J.F. Janik, M.M. Bucko, J. Gosk, A. Twardowski, *RSC Adv.* **5**, 37298 (2015); (b) M. Drygas, J.F. Janik, M. Musial, J. Gosk, A. Twardowski, *Mater. Chem. Phys.*, submitted for publication.

[3] J.F. Janik, M. Drygaś, C. Czosnek, B. Palosz, S. Gierlotka, S. Stelmakh, E. Grzanka, G. Kalisz, A. Świderska-Środa, M. Leszczyński, G. Nowak, R. Czernecki, Polish Patent No. 210651, 29.02.2012, WUP 02/12.

[4] M. Zajac, J. Gosk, E. Grzanka, M. Kaminska, A. Twardowski, B. Strojek, T. Szyszko, S. Podsiadlo, *J. Appl. Phys.* **93**, 4715 (2003).

[5] (a) H. Kato, E. Untersteller, S. Hosaga, G. Kido, W. Treutmann, *J. Magn. Magn. Mater.* **140-144**, 1535 (1995); (b) R.P. Santoro, R.E. Newnham, S. Nomura, *J. Phys. Chem. Solids* **27**, 655 (1966).

[6] M. Zając, J. Gosk, E. Grzanka, S. Stelmakh, M. Palczewska, A. Wysmołek, K. Korona, M. Kamińska, A. Twardowski, *J. Alloys Comp.* **456**, 324 (2008).

[7] J. Gosk, M. Zajac, A. Wolos, M. Kaminska, A. Twardowski, I. Grzegory, M. Bockowski, S. Porowski, *Phys. Rev. B* **71**, 094432 (2005).